

1999

Geometrical Model for a Particle on a Rough Inclined Surface

Giovani L. Vasconcelos
Universidade Federal de Pernambuco

J. J. P. Veerman
Portland State University, veerman@pdx.edu

Let us know how access to this document benefits you.

Follow this and additional works at: https://pdxscholar.library.pdx.edu/mth_fac

 Part of the [Non-linear Dynamics Commons](#)

Citation Details

Vasconcelos, Giovani L. and Veerman, J. J. P., "Geometrical Model for a Particle on a Rough Inclined Surface" (1999). *Mathematics and Statistics Faculty Publications and Presentations*. 149.
https://pdxscholar.library.pdx.edu/mth_fac/149

This Post-Print is brought to you for free and open access. It has been accepted for inclusion in Mathematics and Statistics Faculty Publications and Presentations by an authorized administrator of PDXScholar. For more information, please contact pdxscholar@pdx.edu.

Geometrical model for a particle on a rough inclined surface

Giovani L. Vasconcelos and J. J. P. Veerman

Departamento de Física, Universidade Federal de Pernambuco, 50670-901, Recife, Brazil.

(Accepted in Physical Review E, January 20, 1999)

A simple geometrical model is presented for the gravity-driven motion of a single particle on a rough inclined surface. Adopting a simple restitution law for the collisions between the particle and the surface, we arrive at a model in which the dynamics is described by a one-dimensional map. This map is studied in detail and it is shown to exhibit several dynamical regimes (steady state, chaotic behavior, and accelerated motion) as the model parameters vary. A phase diagram showing the corresponding domain of existence for these regimes is presented. The model is also found to be in good qualitative agreement with recent experiments on a ball moving on a rough inclined line.

PACS number(s): 45.70.-n, 45.50.-j, 05.45.-a

I. INTRODUCTION

Several experimental studies [1–4] have recently been conducted on the problem of a single ball falling under gravity on a surface of controlled roughness. These works have revealed interesting new aspects of granular dynamics that are not yet fully understood. Three distinct dynamical regimes have been identified [1–4] as the tilting angle increases. For small inclinations there is (i) a decelerated regime where the ball always stops, then comes (ii) an intermediate regime where the ball reaches a steady state with constant mean velocity, and for larger inclinations the ball enters (iii) a jumping regime. Computer simulations [2–6] have confirmed these results, particularly those concerning regimes (i) and (ii). A theoretical model [7] has also been proposed in which steady-state solutions (but no detailed dynamics) can be obtained analytically. More recently, a one-dimensional map [8] has been introduced to study the jumping regime. This map in its simplest version is linear, and to obtain non-linear behavior one has to vary spatially the properties of the rough surface [8], in which case the model become inaccessible analytically.

In this Paper we present a model for a single particle moving under the action of gravity on a rough surface of specified shape. Within this setting we will give a detailed analytical description of all possible dynamical regimes. Although the model we study is simplified, its predictions are in good qualitative agreement with the experimental findings.

Roughly speaking, our conclusions are as follows. There is (i) a sharp transition (as the surface inclination increases) from a regime of bounded velocity to one of accelerated motion. Within the region of bounded velocity various dynamical regimes are possible. First there is (ii) a range of inclinations for which the dynamics always has a unique attractor. For higher inclinations two other phases exist: (iii) a region where we have co-existing attractors for the dynamics and (iv) a region where instabilities give rise to chaotic behavior. For a fixed (sufficiently

large) inclination a transition to the chaotic region will take place as the nature of the collisions between the particle and the surface becomes highly inelastic. Although our results are derived here in the context of a simple collision rule, it can be shown [9] that they remain valid for a wide class of restitution laws.

The paper is organized as follows. In Sec. II we describe the model and study in detail its dynamical properties. The main results of this Section are then summarized in the phase diagram shown in Fig. 4. In Sec. III we carry out a comparison between the model predictions and the experimental findings. In particular, we argue that the jumping regime seen in the experiments might correspond to a true chaotic motion, as predicted by the model. Finally, in Sec. IV we collect our main conclusions and present further discussions.

II. THE MODEL

In our model, which is shown in Fig. 1, the rough surface is considered to have a simple staircase shape whose steps have height a and length b . For convenience, we choose a system of coordinates in such a way that the step plateaus are aligned with the x axis and the direction of the acceleration of gravity \mathbf{g} makes an angle ϕ with the y axis. A grain is then imagined to be launched on the top of the ‘staircase’ with a given initial velocity. In what follows, we will be concerned with the problem of a *point* particle falling down this ‘staircase’ and will thus not take into account any effect due to the finite size of the grain. Upon reaching the end of a step plateau, the particle will undergo a ballistic flight until it collides with another plateau located a certain number n of steps below the departure step (e.g., $n = 3$ in Fig. 1). Accordingly, we will refer to the integer n as the *jump number* associated with this flight.

We will assume, for simplicity, that the momentum loss due to collisions is determined by two coefficients of restitution e_t and e_n , corresponding to the tangential and normal directions, respectively. More precisely, if

$\mathbf{v} = (v_x, v_y)$ denote, respectively, the components of the particle velocity parallel and perpendicular to the surface before a collision, then we will take the velocity $\mathbf{v}' = (v'_x, v'_y)$ after the collision to be given by

$$v'_x = e_t v_x, \quad (1a)$$

$$v'_y = -e_n v_y, \quad (1b)$$

where $0 \leq e_t < 1$ and $0 \leq e_n < 1$.

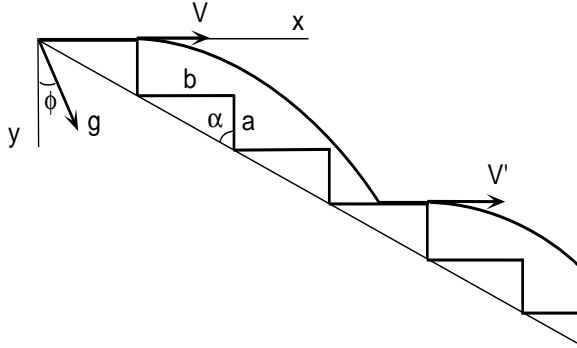


FIG. 1. Model for a single particle moving under gravity on an rough inclined surface.

In the present paper we will for simplicity discuss only the case $e_n = 0$; the advantage being that the model can then be described by a one-dimensional map. When $e_n > 0$ the dynamics is governed by a three-dimensional map, the analysis of which is more complicated and will be left for forthcoming publications [10].

We now derive the equations governing the dynamics of the model presented above. Let us denote by E the kinetic energy of the particle at the moment of departure for a given flight. We write $E = \frac{1}{2}mV^2$, where m is the particle mass and V is the launching velocity at the start of the flight (see Fig. 1). After this flight the particle will first collide with a step below, then slide along this step (recall $e_n = 0$), and finally take off again on another flight with initial kinetic energy E' . We suppose that the main energy loss is due to collisions and so we neglect the energy dissipation as the particle slides along a step, where it then moves with a constant acceleration $g \sin \phi$. Using simple arguments of energy conservation together with the collision conditions (1) and (2), one can write E' in terms of E . The result is

$$E' = \frac{1}{2}m e_t^2 v_x^2 + mg \sin \phi (nb - x), \quad (2)$$

where n is the corresponding jump number for the flight and x is the x -coordinate of the landing point. It takes a simple algebra to show that at the landing point (x, y) we have the following identities:

$$x = \frac{g \sin \phi}{2} T^2 + \sqrt{\frac{2E}{m}} T, \quad (3a)$$

$$y = \frac{g \cos \phi}{2} T^2 = na, \quad (3b)$$

$$v_x = g \sin \phi T + \sqrt{\frac{2E}{m}}, \quad (3c)$$

$$v_y = g \cos \phi T, \quad (3d)$$

where T is the flight time.

It is convenient to introduce a dimensionless energy-like variable:

$$\mathcal{E} = \frac{E}{mga \cos \phi}. \quad (4)$$

Eliminating T from (3) and inserting the result into (2), we obtain that the dynamics of the model in terms of the variable \mathcal{E} is given by the following map:

$$\mathcal{E}' = f(\mathcal{E}, n) = n \left[e_t^2 \left(\sqrt{\mathcal{E}/n} + t \right)^2 + t \left(\tau - t - 2\sqrt{\mathcal{E}/n} \right) \right]. \quad (5)$$

where we have for conciseness introduced the notation

$$t = \tan \phi, \quad (6)$$

$$\tau = b/a. \quad (7)$$

The parameter τ above can be viewed as a measure of the surface roughness, with $\tau^{-1} = 0$ corresponding to a perfectly smooth surface. As for the inclination parameter t , we need to consider only the interval $0 < t < \tau$ for which non-trivial motion occurs. (Clearly, for $t < 0$ the particle will always come to a rest, whereas for $t > \tau$ the particle undergoes a free fall without ever colliding again with the ramp.)

The flight jump number n appearing in Eq. (5) is determined from the energy \mathcal{E} according to the following condition: n is equal to the smallest integer such that $nb - x \geq 0$ or, alternatively,

$$n(\tau - t) - 2\sqrt{n\mathcal{E}} \geq 0. \quad (8)$$

This means that \mathcal{E} falls within the interval I_n :

$$\mathcal{E} \in I_n(t) \equiv \left[\frac{1}{4}(n-1)(\tau-t)^2, \frac{1}{4}n(\tau-t)^2 \right]. \quad (9)$$

Thus the function $f(\mathcal{E}, n)$, as defined by Eqs. (5) and (9), exhibits jump discontinuities at energy values $\mathcal{E} = \frac{1}{4}n(\tau-t)^2$, but each of its branches is smooth. This is illustrated in Fig. 2, where we graph the function (5) for $e_t = 0.7$, $\tau = 3.7$, and several values of the inclination t ,

For later use, we note here that the average velocity \bar{V} between two consecutive flights is given by

$$\bar{V} = \frac{nL}{T + (\sqrt{2E'/m} - e_t v_x)/g \sin \phi}, \quad (10)$$

where $L = \sqrt{a^2 + b^2}$ and the second term in the denominator corresponds to the time during which the particle

moves on the ramp (see Fig. 1). If we now introduce a dimensionless mean velocity

$$\bar{v} = \frac{\bar{V}}{\sqrt{ag \cos \phi}}, \quad (11)$$

then Eq. (10) becomes

$$\bar{v} = \frac{t\sqrt{n(1+\tau^2)/2}}{(1-e_t)t + \sqrt{\mathcal{E}'/n} - e_t\sqrt{\mathcal{E}/n}}. \quad (12)$$

In order to study the dynamical properties of the map above, we must first investigate the existence of fixed points. If we denote by \mathcal{E}_n a fixed point with a jump number n , then \mathcal{E}_n will be the solution to the equation

$$\mathcal{E}_n = f(\mathcal{E}_n, n). \quad (13)$$

In view of the homogeneity of the function $f(\mathcal{E}, n)$ [see Eq. (5)] we write

$$\mathcal{E}_n = n[z_0(t)]^2, \quad (14)$$

where the quantity $z_0(t)$ no longer bears any dependence on n . Using Eqs. (5) and (14), Eq. (13) becomes

$$(z_0 + t)^2 = e_t^2(t + z_0)^2 + \tau t, \quad (15)$$

whose positive solution is

$$z_0(t) = -t + \sqrt{\frac{\tau t}{1 - e_t^2}}. \quad (16)$$

Now a fixed point \mathcal{E}_n , as given in Eqs. (14) and (16), will exist if and only if $\mathcal{E}_n \in I_n(t)$, where the interval $I_n(t)$ is defined in (9). Thus, as t increases, a fixed point with jump number n will be born when \mathcal{E}_n equals the left endpoint of I_n . Comparing Eqs. (9), (14) and (16), we see that this happens at an inclination t_n such that

$$z_0(t_n) = -t_n + \sqrt{\frac{\tau t_n}{1 - e_t^2}} = \frac{1}{2} \sqrt{1 - \frac{1}{n}} (\tau - t_n). \quad (17)$$

This equation is quadratic in $\sqrt{t_n}$ and can thus be easily solved. However, we shall not bother to give the result here and will simply mention a few important facts that follow from Eq. (17). First, we note that $t_1 = 0$ so that a fixed point with jump number $n = 1$ is always born at $t = 0$. Then, as t increases, fixed points with successively higher n will appear in an increasing sequence of inclinations $\{t_n\}_{n=1}^{\infty}$. Finally, we have that for $t > t_{\infty}$, where $t_{\infty} = \lim_{n \rightarrow \infty} t_n$, all fixed points cease to exist. Setting $n = \infty$ in Eq. (17) we obtain for the limit point t_{∞} :

$$t_{\infty} = \tau \frac{1 - e_t}{1 + e_t}. \quad (18)$$

The appearance of this sequence of fixed points can perhaps be best visualized by referring to Fig. 2, where we

plot the function $f(\mathcal{E}, n)$ at increasing values of t , with e_t and τ kept fixed. For small t (lower-most curve in Fig. 2) there is only one intersection with the 45° line, corresponding to the fixed point with the $n = 1$. As t increases fixed points with successively higher n appear (second curve from the bottom). At $t = t_{\infty}$ there are infinitely many such fixed points (second curve from the top) and after this all of them cease to exist (uppermost curve).

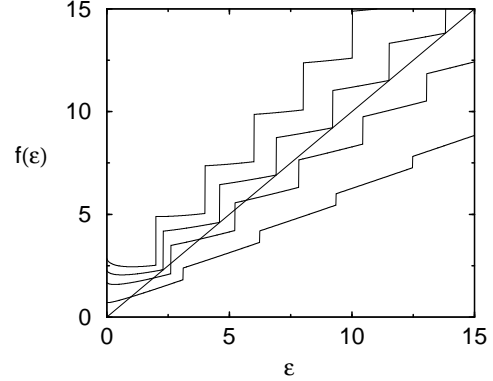


FIG. 2. One-dimensional map $f(\mathcal{E}, n)$ for $e_t = 0.7$, $\tau = 3.7$ and $t = 0.2, 0.5, 0.7, 0.9$ (from the bottom up).

One can also show that for $t > t_{\infty}$ we always have $f(\mathcal{E}, n) > \mathcal{E}$, whereas for $0 < t < t_{\infty}$ there exists an energy \mathcal{E}^* such that $f(\mathcal{E}, n) < \mathcal{E}$ for $\mathcal{E} > \mathcal{E}^*$ (see, e.g., Fig. 2). We thus conclude that for $t > t_{\infty}$ the particle velocity will become unbounded for any initial condition, whereas for $0 < t < t_{\infty}$ the velocity remains always bounded. In other words, at the critical inclination $t = t_{\infty}$ there is a sharp transition (independent of initial conditions) from a regime of bounded velocity to accelerated motion. In the region of bounded velocity, several dynamical regimes are possible, depending on the stability of the fixed points, as discussed below.

The stability of a fixed point \mathcal{E}_n is determined by the parameter $\lambda = f'(\mathcal{E}_n, n)$, where the prime denotes derivative with respect to \mathcal{E} , so that if $|\lambda| < 1$ ($|\lambda| > 1$) the fixed point is stable (unstable) [11]. Using Eqs. (5), (14) and (16), we obtain for the derivative λ at the fixed point:

$$\lambda(t) = 1 - \frac{1 - e_t^2}{1 - \sqrt{(1 - e_t^2)t/\tau}}. \quad (19)$$

Notice that λ does not depend on n , thus implying that all existing fixed points \mathcal{E}_n (for given values of the model parameters) have the same stability properties. Moreover, since λ is always smaller than unity, we see that instability can occur only if $\lambda(t) < -1$. Let us then denote by t_{inst} the inclination such that $\lambda(t_{\text{inst}}) = -1$. From Eq. (19) we obtain that

$$t_{\text{inst}} = \tau \frac{(1 + e_t^2)^2}{4(1 - e_t^2)}. \quad (20)$$

Thus the fixed points are stable for $t < t_{\text{inst}}$ and unstable for $t > t_{\text{inst}}$.

If the fixed points are stable, the dynamics of the map will in general be attracted to one of the existing fixed points. For example, in the region of parameters such that $0 < t < t_2 < t_{\text{inst}}$ the particle will almost always reach a periodic motion where the particle falls by one step at a time, since in this case only the fixed point with $n = 1$ exists and is stable [12]. On the other hand, for $t_2 < t < t_{\text{inst}}$ there are co-existing stable fixed points, in which case the final state (i.e., the fixed points to which the dynamics is attracted) will depend on the initial condition. Once the system has reached a given fixed point \mathcal{E}_n the particle will accordingly be moving with a constant mean velocity \bar{v}_n whose value can be readily obtained by inserting Eqs. (14) and (16) into Eq. (12):

$$\bar{v}_n = \left[\frac{n(1 + \tau^2)t}{2t_\infty} \right]^{1/2}. \quad (21)$$

When the fixed points are unstable ($t_{\text{inst}} < t < t_\infty$), the particle motion becomes very irregular and no stationary (periodic) regime is ever reached. This is illustrated in Fig. 3, where we plot the jump number n as a function of time (iteration step) for two orbits in the region where the fixed points are unstable. In this figure we clearly see that the jump number fluctuates erratically around a mean value. We have computed the Lyapunov exponent for several values of parameters in the region of unstable fixed points and have found it to be positive for all cases studied, thus indicating that the motion is indeed chaotic in this region.

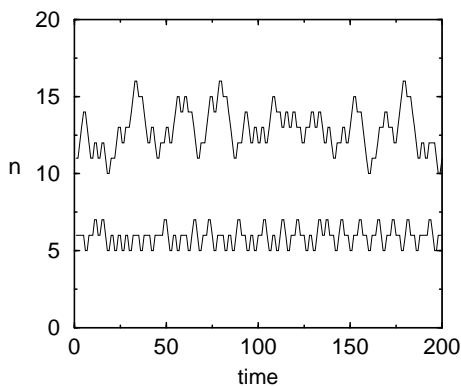


FIG. 3. The jump number n as a function of time (measured in iteration steps) in the chaotic regime. Here $e_t = 0.35$, $\tau = 3.73$, and $t = 1.65$ (lower orbit), 1.74 (upper orbit).

The different dynamical regimes displayed by the model above can be conveniently summarized in terms of a “phase diagram” in the parameter space $(e_t, t/\tau)$, as shown in Fig. 4. In this figure we plot the curves corresponding to t_∞ (solid line) and t_{inst} (dashed line) given by Eqs. (18) and (20), respectively. Also plotted is the

curve representing the inclination t_2 (dot-dashed line) at which the fixed point with $n = 2$ first appears. Thus in terms of the existence/stability of the fixed points the model displays the following four regions: (i) for $0 < t < \min(t_2, t_{\text{inst}})$ there is a unique stable fixed point, namely, that with $n = 1$; (ii) for $t_2 < t < \min(t_{\text{inst}}, t_\infty)$ there are multiple stable fixed points (at least those with $n = 1$ and $n = 2$); (iii) for $t_{\text{inst}} < t < t_\infty$ all existing fixed points are unstable and chaotic motion is observed; (iv) for $t > t_\infty$ no fixed point exists and the motion becomes accelerated.

Another interesting feature in Fig. 4 is the fact that the chaotic regime appears when the collisions are highly inelastic (i.e., small e_t). In particular, for $e_t > \sqrt{2} - 1$ (at which point t_{inst} equals t_∞) the fixed points remain stable over their entire domain of existence. (The results shown in Fig. 4 are qualitatively different from the behavior seen in the model studied in Ref. [8], where chaotic motion appears as the restitution coefficient increases.)

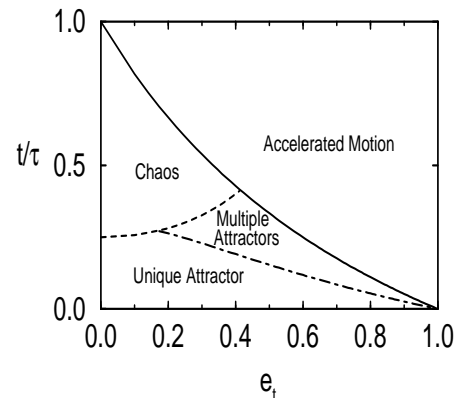


FIG. 4. Phase diagram for the model. The solid line corresponds to t_∞ , the dashed line to t_{inst} , and the dot-dashed line to t_2 .

III. COMPARISON WITH EXPERIMENTS

In this section we wish to compare our model with recent experimental studies of a single ball moving under gravity on a rough inclined surface. In these experiments, first performed by Jan *et al.* [1] and later expanded by Ristow *et al.* [4], a rough surface was constructed by gluing steel spheres of radius r on a L-shaped flume. Another steel sphere of radius R was then launched with a small initial velocity and its subsequent motion analyzed. As the surface inclinations increases, the following three regimes are observed [4]: for small inclinations the bead always stops (regime A), then comes a range of inclinations for which the ball reaches a steady state with constant mean velocity (regime B), and beyond this point the ball starts to jump (regime C). In Fig. 5 we

show data taken from Ref. [4] for the ball mean velocity \bar{V} as a function of $\sin\theta$, where θ is the inclination angle with respect to the horizontal direction. As discussed in Ref. [4], the change in trend observed in the data as θ increases (for a given value of R/r) marks the beginning of the jumping regime.

The regime B seen in the experiments corresponds in our model to a stable fixed point with $n = 1$, for in this case the particle reaches a periodic motion where it falls one step at a time (as in the experiments). In order to compare our model more closely with the experiments let us first express the mean velocity \bar{V}_1 (at the fixed point $n = 1$) in terms of the angle θ , where $\theta = \phi + \pi/2 - \alpha$ (see Fig. 1). Setting $n = 1$ in Eq. (21), returning to dimensionful units via Eq. (11), and expressing the final result in terms of θ , we obtain

$$\bar{V}_1 = \left[\frac{Lg(1 + e_t)}{2(1 - e_t)} \right]^{1/2} \sqrt{\sin\theta - \tau^{-1} \cos\theta}. \quad (22)$$

(We remark parenthetically that a similar expression can be obtained heuristically if one introduces an effective sliding friction in addition to inelastic collisions; see Refs. [1,4]. Our formula follows however from a pure collision model.)

We have fitted the expression (22) to the experimental data shown in Fig. 5 — the corresponding results being displayed as solid curves in this figure. In our fitting procedure, we took $L = 2r = 1$ cm [4], $g = 980$ cm/s², and best-fitted the parameters τ and e_t for each data set considering *only* points in regime B. As we see in Fig. 5, the model prediction for the dependence of \bar{V} with θ is in a good agreement with the experimental data (in regime B).

The jumping regime observed in the experiments, on the other hand, would correspond in our model to the region of unstable fixed points, since in this case the particle jumps erratically never reaching a steady state (see Fig. 3). This analogy might then provide a possible explanation for the change in trend observed in the experimental data for large inclinations. To see this, consider the region of small e_t in the phase diagram shown in Fig. 4. As the inclination t increases (for a given e_t) the system goes from a region of stable periodic motion (with $n = 1$) to a regime of chaotic jumps, in close resemblance to the experimental transition from steady-state to the jumping regime.

To probe this analogy further, we illustrate in Fig. 6 the behavior predicted by the model for the mean velocity \bar{V} as a function of $\sin\theta$ in the region of small e_t . In this figure, the solid curve corresponds to the expression (22) for \bar{V}_1 , up to the point where the fixed point goes unstable, and the crosses are computed values of \bar{V} in the ensuing chaotic regime. Comparing Fig. 6 with Fig. 5, we see that the change in behavior predicted by the model at the onset of instability is in qualitative agree-

ment with what is observed in the experiments (for small values of R/r) as the ball enters the jumping regime. Of course, more detailed experiments are necessary to verify whether chaotic motion does indeed take place in the jumping regime.

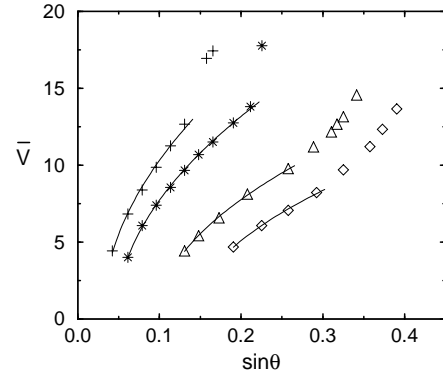


FIG. 5. Mean velocity \bar{V} (cm/s) as a function of $\sin\theta$. Points are experimental data taken from Ref. [4] for $R/r = 2$ (+), 1.5 (*), 1 (Δ), 0.8 (\diamond). Solid curves are theoretical fits [Eq. (22)], ending near the last data point considered in the fit. Fitted parameters are $(e_t, \tau) = (0.72, 33.18)$, $(0.64, 21.09)$, $(0.41, 10.17)$, $(0.27, 7.07)$, from left to right.

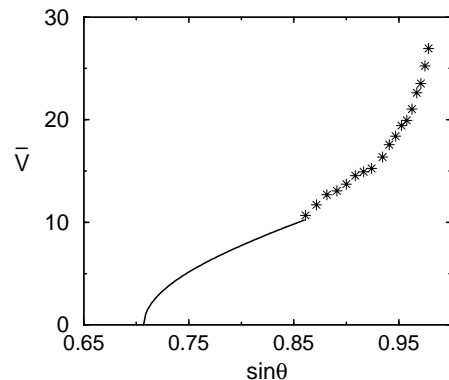


FIG. 6. Same as figure 5 for our model with $e_t = 0.1$ and $\tau = 1$. The solid curve corresponds to Eq. (22) whereas the stars give the computed mean velocity in the chaotic regime.

IV. CONCLUSIONS

We have studied a simple geometrical model for the gravity-driven motion of a single particle on a rough inclined line. In our model the rough line was chosen to have a regular staircase shape and a simple collision law was adopted. With these simplifications the dynamics is described by a one-dimensional map that is quite amenable to analytical treatment. Summarizing our findings, we have seen that our model displays the following

four dynamical regimes:

1. for $0 < t < \min(t_2, t_{\text{inst}})$ there is a unique stable fixed point.
2. for $t_2 < t < \min(t_{\text{inst}}, t_\infty)$ the system has multiple stable fixed points.
3. for $t_{\text{inst}} < t < t_\infty$ the fixed points are unstable and the dynamics is chaotic.
4. for $t > t_\infty$ no fixed point exists and the motion becomes accelerated.

Here the parameter t measures the surface inclination and the quantities t_2 , t_{inst} , and t_∞ separating the different regimes are given in terms of the other two model-parameters, namely, the restitution coefficient e_t and the roughness parameter τ . These regimes are indicated in the phase diagram shown in Fig. 4. Furthermore, it can be shown [9] that the above conclusions, which were derived in the context of a simple collision rule, remain valid for a wide class of tangential restitution laws.

Despite its simplicity, our model does provide a theoretical framework within which the generic behavior seen in experiments on a ball moving on a rough surface can be qualitatively understood. For example, the model successfully predicts the existence of several dynamical regimes that are also observed in the experiments. In particular, the predicted functional dependence of the mean velocity with the inclination angle θ (in the steady-state regime) is in good agreement with the experiments. Moreover, the model provides a possible explanation for the change in trend seen in the experimental data as the ball enters the jumping regime. We have suggested that this jumping regime might correspond to a chaotic motion, as so happens in the model. Clearly, more experimental studies are required to investigate this interesting possibility.

This work was supported in part by FINEP and CNPq.

- [6] S. Dippel, G. G. Batrouni, and D. E. Wolf, Phys. Rev. E **54**, 6845 (1996); **56**, 3645 (1997).
- [7] C. Ancey, P. Evesque, and P. Coussot, J. Phys. I France **6**, 725 (1996).
- [8] A. Valance and D. Bideau, Phys. Rev. E **57**, 1886 (1998).
- [9] J. J. P. Veerman and G. L. Vasconcelos, preprint.
- [10] C. G. Alves-Neto, G. L. Vasconcelos, and J. J. P. Veerman, in preparation.
- [11] E. Ott, *Chaos in Dynamical Systems* (Cambridge University Press, New York, 1993).
- [12] When t is very close to t_{inst} the system may enter a chaotic regime for certain initial conditions, while converging to the fixed point for others.

-
- [1] C. D. Jan, H. W. Shen, C. H. Ling, and C. I. Chen, in *Proceedings of the 9th Conference of Engineering Mechanics, College Station, Texas*, edited by L. D. Lutes and J. M. Niedzwecki (American Society of Civil Engineers, 1992), pp. 768.
 - [2] F.-X. Rigidel, R. Julien, G. H. Ristow, A. Hansen, and D. Bideau, J. Phys. I France **4**, 261 (1994).
 - [3] F.-X. Rigidel, A. Hansen, and D. Bideau, Europhys. Lett. **28**, 13 (1994).
 - [4] G. H. Ristow, F.-X. Rigidel, and D. Bideau, J. Phys. I France **4**, 1161 (1994).
 - [5] G. G. Batrouni, S. Dippel, and L. Samson, Phys. Rev. E **53**, 6496 (1996).